VLA Test Memorandum # 180

Corrections of Beam Squint for the Improvement of Circular Polarization Measurements with the VLA

Angelos Vourlidas

Department of Physics
N. Mexico Institute of Mining & Technology
Soccoro, NM 87801

and

T. Bastian

National Radio Astronomy Observatory

Introduction

In this memorandum we report some initial efforts to correct maps of the Sun and other cosmic sources for the effects of the VLA *beam squint* (Clark, 1976; Thompson, 1976). Because of the feed design on VLA antennas, the phase centers for the RCP and LCP beams are displaced from the feed phase center in opposite directions. The magnitude of the offset between the RCP and LCP beams amounts to $\approx 3\%$ of the HPBW of the primary beam. As a result, maps are corrupted by a polarization gradient across the field of view. A good discussion of this and other outstanding problems concerning the measurement of, and correction for, instrumental polarization of the VLA is given in Holdaway, Carilli and Owen (1992).

The memo is organized as follows: In Sect. 1, we present recent measurements and improved fits for the VLA primary beam parameters. In Sect. 2 we describe a first order correction for the beam squint which is easily implemented in the map domain. Additional problems with the beam squint are discussed in Sect. 3 and a strategy for dealing with them is described. Future work in this area is briefly discussed in Sect. 4.

1. VLA Primary Beam Parameters

Any attempt to correct for the beam squint requires well-determined RCP and LCP beams. The primary beam was mapped in three bands – L, C, and X – out to the half-power point using the 'raster mode' (Sowinski, 1991). The following table

TABLE 1

Raster Observations

Frequency (GHz)	Step (arcmin*GHz)
1.465	4.6636
1.515	4.8228
4.835	6.9366
4.885	6.8656
8.415	4.5704
8.465	4.5975

summarizes the observed frequencies and the sampling interval for each step of the 9×9 raster array.

We have performed a 2-D polynomial least-squares fit for each **inverse** beam and polarization, using (arcmin*GHz) as the independent parameter (see Napier and Rots 1982). We found that fourth degree polynomial gives the best results. There are no significant differences in the fit for different frequencies within the same band so, for example, the fit of the 1.465 GHz beam can be used for all frequencies within the band. Fig. 1 - Fig. 3 show the fitted beams and the normalized error (err = (fitted - observed)/observed) as a 1-D plot for each polarization. The coefficients of the fit are as follows:

FIT RESULTS FOR L-BAND (N=4)

```
RCP COEFFICIENTS
      1.00827   0.00262978   0.00127411  2.11441e-06  1.83910e-06
  0.000691144  6.41503e-05 -6.94823e-06 -1.17909e-07  1.50042e-08
   0.00133280  1.36266e-05  3.57478e-06 -3.91422e-08 -1.38584e-09
  8.01254e-06  7.96788e-08  2.60065e-08  3.82687e-10  7.38254e-12
  1.61537e-06 -7.96192e-09 -2.27407e-09  9.46515e-11  1.99527e-11
LCP COEFFICIENTS
      1.00913  -0.00128194   0.00130906 -1.11687e-05  1.68665e-06
 -0.00347176  7.15774e-05 -1.16079e-05 -1.34837e-07  1.36665e-09
   0.00136361  3.49846e-06  3.62342e-06 -4.39466e-08 -1.38732e-09
 -3.47027e-06  2.62853e-08  1.06905e-08  4.76901e-10 -6.07289e-11
  1.54337e-06 -5.44631e-09 -2.29799e-09  1.25192e-12  1.94003e-11
```

FIT RESULTS FOR C-BAND (N=4)

```
RCP COEFFICIENTS
      1.04177 -5.44776e-05  0.000809367 -1.36092e-05  3.36004e-06
  0.000247584  5.21085e-07 -4.14707e-06 -1.12217e-07  2.07156e-08
```

```
 0.000916967  1.08705e-06  1.38169e-06 -4.41379e-08  1.44213e-10
-2.37416e-05 -2.51500e-08  1.07145e-08  8.16228e-10 -2.06279e-10
 2.90868e-06 -7.68386e-09 -1.32603e-09  4.01331e-11  2.79089e-11
LCP COEFFICIENTS
      1.04191 -1.57472e-05  0.000784826  2.34786e-05  3.44011e-06
  0.00109261  1.67232e-05  4.06325e-07 -2.04163e-07  9.47732e-10
 0.000911780  9.68727e-06  1.79476e-06 -5.49472e-08 -9.78472e-10
-5.10580e-06 -7.83088e-08 -1.59087e-09  7.54236e-10 -9.55871e-12
 2.90784e-06 -5.48684e-08 -2.77973e-09  3.98184e-10  3.18085e-11

                    FIT RESULTS FOR X-BAND (N=4)

RCP COEFFICIENTS
     0.999195 -0.000575957   0.00135281 -5.82389e-07  1.09347e-06
 -0.00242586 -0.000173919  1.09164e-06  4.97243e-07 -1.99788e-09
  0.00137307  1.82766e-07  2.08234e-06  9.62630e-09  9.60632e-10
 2.01289e-06 -9.31237e-08 -2.51069e-09  2.71084e-10  5.83343e-11
 1.08296e-06 -1.44145e-08  1.65297e-09  4.94997e-11  6.94388e-12
LCP COEFFICIENTS
      1.00015   0.00539513   0.00136717  1.40013e-05  1.19870e-06
 -0.00148270 -0.000170886  1.51946e-06  4.74270e-07  2.40579e-09
  0.00137244  8.73413e-06  1.99764e-06  3.25662e-08  1.70853e-09
 4.14692e-06 -1.08380e-07 -2.42596e-09  7.56568e-10  8.26677e-11
 1.08997e-06 -6.48877e-09  2.00722e-09  1.03744e-10  6.44915e-12
```

The above fits can be applied to VLA maps using an algorithm that explicitly corrects maps for the RCP and LCP beam response (e.g., task **PBCOR** in *AIPS*). At the moment, **PBCOR** uses a 1-D fit (Napier and Rots 1982) which is less CPU intensive. However, for moderate data sets the use of the full 2-D polynomial fits could be used.

2. Correction for the Induced Polarization Gradient

Radio sources which are intrinsically circularly polarized include the Sun, planets, stars, and astronomical masers. The circularly polarized radiation is conventionally described using the Stokes V parameter or the "degree of circular polarization" ($\rho_C = V/I$, where I is the total intensity). A fairly simple correction may be applied to the latter quantity.

Suppose that the primary beam is taken as Gaussian with a HPBW of θ_{HPBW}. Let (x_o, y_o) represent the offset of the RCP beam due to the beam squint. Then we can write the RCP and LCP beams, $A_R(x,y)$ and $A_L(x,y)$, as

$$\mathcal{A}_R(x,y) = \mathcal{A}_o\, e^{-\alpha^2\left[(x-x_o)^2+(y-y_o)^2\right]}$$

$$\mathcal{A}_L(x,y) = \mathcal{A}_o\, e^{-\alpha^2\left[(x+x_o)^2+(y+y_o)^2\right]} \tag{1}$$

where $\alpha^2 = 4\ln 2/\theta^2_{HPBW}$. Expanding, one has

$$\begin{aligned}\mathcal{A}_R(x,y) &= \mathcal{A}_o\, e^{-\alpha^2(x^2+y^2)}\, e^{-\alpha^2(x_o^2+y_o^2)}\, e^{2\alpha^2(xx_o+yy_o)} \\ &\approx \mathcal{A}_o\, e^{-\alpha^2(x^2+y^2)}\, e^{-\alpha^2(x_o^2+y_o^2)}\, \left(1+2\alpha^2\,(xx_o+yy_o)\right) \\ &= \mathcal{A}'\,(x,y)\, \left(1+2\alpha^2\,(xx_o+yy_o)\right)\end{aligned} \tag{2}$$

A similar relation holds for the LCP beam, with the final term on the RHS being $1-2\alpha^2(xx_o+yy_o)$. If the "true" Stokes I parameter is given by $I(x,y) = \frac{1}{2}(RR(x,y)+LL(x,y))$ and $V(x,y) = \frac{1}{2}(RR(x,y)-LL(x,y))$, where $RR(x,y)$ and $LL(x,y)$ represent the "true" source brightness distribution in RCP and LCP, respectively, then the measured Stokes I parameter can be written $I' = \frac{1}{2}(\mathcal{A}_R(x,y)RR(x,y)+\mathcal{A}_L(x,y)LL(x,y))$. Similarly, the measured Stokes V is $V' = \frac{1}{2}(\mathcal{A}_R(x,y)\,RR(x,y)-\mathcal{A}_L(x,y)LL(x,y))$. The measured degree of circular polarization can then be written

$$\rho_c' = \frac{V'\,(x,y)}{I'\,(x,y)} = \frac{V\,(x,y)+I\,(x,y)\,g\,(x,y)}{I\,(x,y)+V\,(x,y)\,g\,(x,y)} \tag{3}$$

where $g(x,y) = 2\alpha^2(xx_o+yy_o)$. Rearranging terms in Eqn. 3, one obtains the corrected degree of polarization:

$$\rho_c = \frac{V\,(x,y)}{I\,(x,y)} = \frac{V'\,(x,y)-I'\,(x,y)\,g\,(x,y)}{I'\,(x,y)-V'\,(x,y)\,g\,(x,y)} \tag{4}$$

Correction of V' and I' separately is not desirable in this prescription to the extent that the Gaussian $\mathcal{A}'(x,y)$ is not an adequate model of the primary beam shape:

$$V\,(x,y) = \frac{V'\,(x,y)-I'\,(x,y)*g\,(x,y)}{\left(1-g\,(x,y)^2\right)\mathcal{A}'\,(x,y)} \tag{5}$$

and

$$I\,(x,y) = \frac{I'\,(x,y)-V'\,(x,y)*g\,(x,y)}{\left(1-g\,(x,y)^2\right)\mathcal{A}'\,(x,y)}. \tag{6}$$

Suppose now that an unpolarized source is observed (V(x,y)=0). From Eqn. 3, $\rho_c' = g(x,y)$. To the extent that ρ_c' is well-approximated by a plane at some orientation(see Fig. 4), Eqn. (4) can be used to correct the degree of circular polarization

measured at some instant in time. In practice, observations are carried out over an extended period of time. The polarization gradient therefore rotates on the sky. Hence, an appropriately weighted average of $g(x,y)$ must be employed in Eqn. 4 to reflect its changing orientation in time.

An *AIPS* task (**RCCOR**) has been written to perform such a correction. We have used the raster data described in Sect. 2 to form ρ_c' for each band and find that, in each case, $\rho_c'(x,y)$ is well-approximated by a plane at some band-dependent orientation. We have fit a 2-D first degree polynomial to $\rho_c'(x,y)$ in each band to infer $g(x,y)$ referenced to local noon. Rotation of $g(x,y)$ is affected through the application of an appropriate rotation matrix.

The results of the polynomial fits to $\rho_c'(x,y)$ are as follows:

```
                    FIT RESULTS FOR L-BAND (N=1)
RHO_C COEFFICIENTS
  0.000471546 -6.18860e-05
 -6.02346e-05 -2.24317e-09

                    FIT RESULTS FOR C-BAND (N=1)
RHO_C COEFFICIENTS
  0.000661990  0.000325438
  0.000181590  8.47022e-09

                    FIT RESULTS FOR X-BAND (N=1)
RHO_C COEFFICIENTS
   0.00120512  0.000481342
  7.53175e-05  6.19907e-08
```

The above numbers are the coefficients in the equation $\rho_c = a_{11} + a_{12} * x + a_{21} * y + a_{22} * xy$, where x, y are the coordinates offsets, in arcsec, in AZ and EL, respectively, at *local noon*. Note that $\arctan(a_{12}/a_{21})$ gives the orientation of the polarization gradient (i.e., the offset vector between the RCP and LCP beam response) and the offset itself is given by $\sqrt{a_{12}^2 + a_{21}^2} \times C$, where $C = 353.2/\nu_{GHz}^2(\mathrm{arcmin}^2)$. The position angle of the squint is essentially the position angle of the corresponding feed and the beam offset is orthogonal to that angle. The positions are measured clockwise from the upper leg of the quadropod. If we calculate these parameters for the above measurements we get the following values, where the percent beam offset with respect to the FWHP is given in the parentheses.

TABLE 2

Derived Squint Parameters

VLA Band	Squint Angle (degrees)	Squint Offset (arcsec)
L	$225^{\circ}.77$	$51''.16$ (2.8%)
C	$29^{\circ}.16$	$20''.27$ (3.7%)
X	$81^{\circ}.11$	$8''.75$ (2.7%)

These values correspond to mean for all antennas. The same quantities have been plotted for each antenna in Fig. 5 and Fig. 6 in both the L and X bands.

The statistics for these measurements are shown in the following table. We see that the squint for each antenna is very close to the values obtained for the whole array (Table 2). The same conclusion was reached in Holdaway, Carilli and Owen (1992) where they analyzed data from all the VLA frequency bands. Therefore, we are safe in assuming that the beam squint is essentially identical for all antennas.

TABLE 3

Squint Parameters for individual antennas

VLA Band	Average Position Angle (deg)	Mean Offset (arcsec)
L	$225^{\circ}.93 \pm 1^{\circ}.58$	$52''.14 \pm 1''.47$
X	$81^{\circ}.42 \pm 0^{\circ}.86$	$8''.68 \pm 0''.14$

3. Additional Considerations

The rotation of the primary beam on the sky introduces another problem: the measured circularly polarized intensity of a given source shows an apparent variation with time as do its sidelobes (see also sect. 6 in Holdaway, Carilli and Owen, 1992). As a consequence, the dynamic range of a given map be limited (to an extent which depends on the details of the brightness distribution). It should also be noted that, for a source like the Sun, much of the temporal variability observed is not due solely to primary beam rotation, but is intrinsic to the source itself. A possible way to deal with these problems is through the following algorithm suggested by T. Cornwell (1992) and implemented as an *AIPS Run* file by A. Vourlidas. The algorithm works as follows:

Step 1. A model of the source is computed and subtracted from the UV data (tasks **APCLN** and **UVSUB**).

Step 2. The UV data is split into time blocks during which the change in parallactic angle is small (e.g, $\Delta\phi \approx 10°$); these data sets are imaged with **HORUS**.

Step 3. A deep CLEAN of the residual is then performed and the model clean components are added back to the individual maps (tasks **APCLN** and **RSTOR**).

Step 4. The resulting maps are weighted according to their rms noise and summed (task **LTESS**) to form the final corrected map.

There are a couple of considerations that one should keep in mind before adopting this procedure. First, the use of many separate deconvolutions can lead to image *degradation* which is mostly due to the sparse *u-v* coverage of the individual blocks in comparison with the combined UV data (Appendix. D in Holdaway, Carilli and Owen (1992)). This effect can be remedied to a certain degree by a careful choice of the uv limits during the FFT stage of the procedure. Second, the algorithm is designed to reduce the sidelobe level caused by the temporal variation of sources due to the rotating primary beam and its associated squint, as well as that due to intrinsic variability of the source – it does not correct for the squint itself. However, it has been demonstrated that this procedure, coupled with the application of the task **RCCOR** described in the previous section, can lead to a significant improvement in the dynamic range of a given map and in the accuracy of the measured degree of circular polarization (Vourlidas 1993; Fig. 7).

Conclusions & Future Work

We have reported preliminary attempts to investigate and correct the effects of the VLA beam squint. However, there is still room for improvement of circular polarization measurements. For example, the limitations introduced by sidelobes caused by the apparent variability of source polarization(Sect. 3) can perhaps be better dealt with through a simultaneous deconvolution scheme (Holdaway, Carilli and Owen, 1992; Cornwell and Evans, 1985). This is currently under investigation.

References

Clark, B. G. 1976, "A Rough Measurement of the Polarization Properties of the VLA Antenna", VLA Test Memo 111.

Cornwell, T. J., and Evans, K. F., *Astr. Ap*, 143, 77, 1985.

Cornwell, T. J. 1992, *private communication.*

Holdaway, M. A., Carilli, C. L., and Owen, F. 1992, "Possible Algorithms to Improve VLA's Polarization Performance", VLA Scientific Memo 163.

Napier, P. J., and Rots, A. H. 1982, "VLA Primary Beam Parameters", VLA Test Memo 134.

Sowinski, K. 1991, "Use of the 'Raster Mode' at the VLA", VLA Computer Memo 182.

Thompson, A. R. 1976, "The Effect of Beam Offsets on Polarization Measurements", VLA Scientific Memo 125.

Vourlidas, A. 1993, "The Structure of Solar Active Regions as Inferred from Multifrequency VLA Observations", Ms Thesis, N. Mexico Inst. of Min. & Tech.

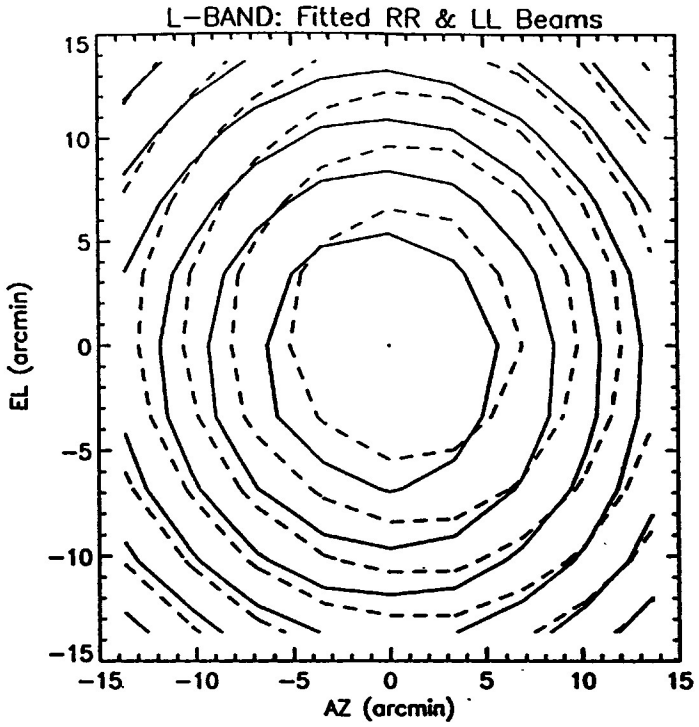

a)

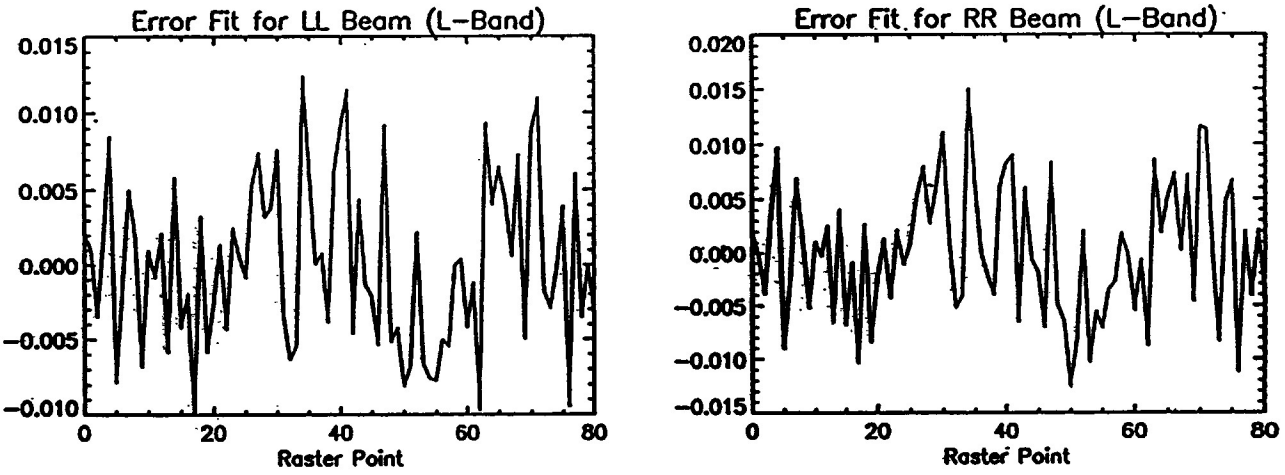

b)

Figure 1: (a) Circular Polarization beams for L-Band. (b) Normalized error for LL and RR beams.

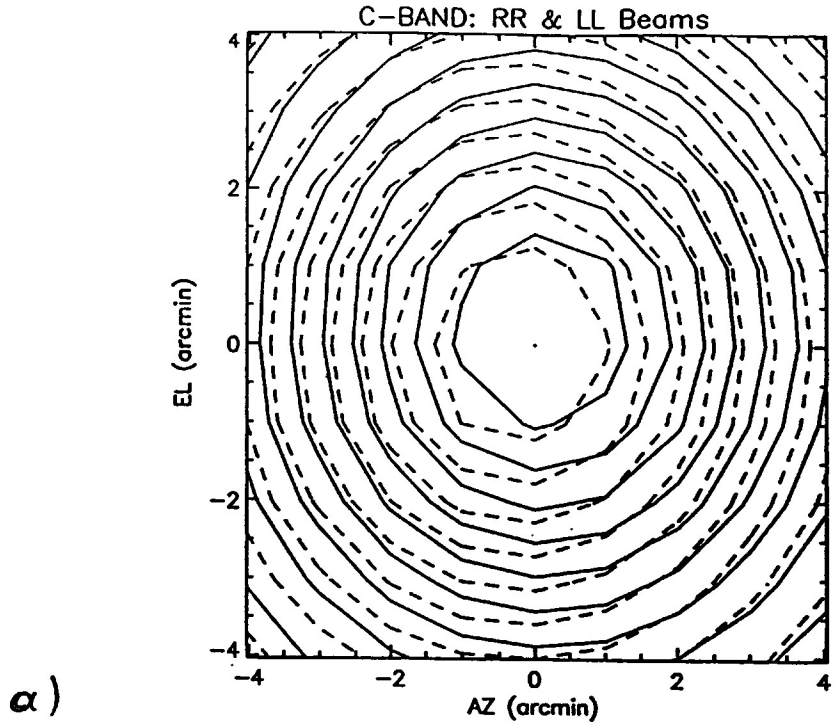

a)

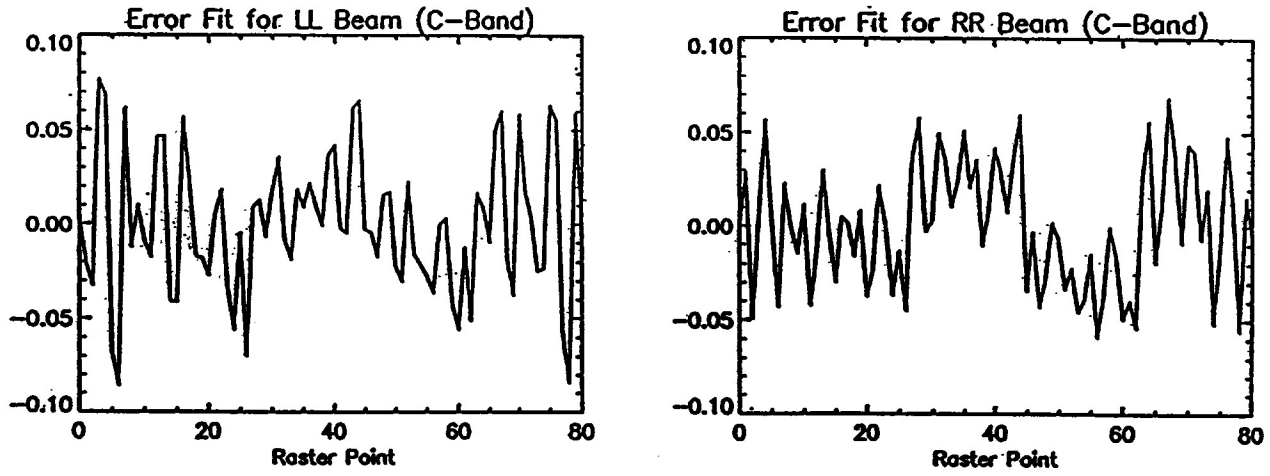

b)

Figure 2: (a) Circular Polarization beams for C-Band. (b) Normalized error for LL and RR beams.

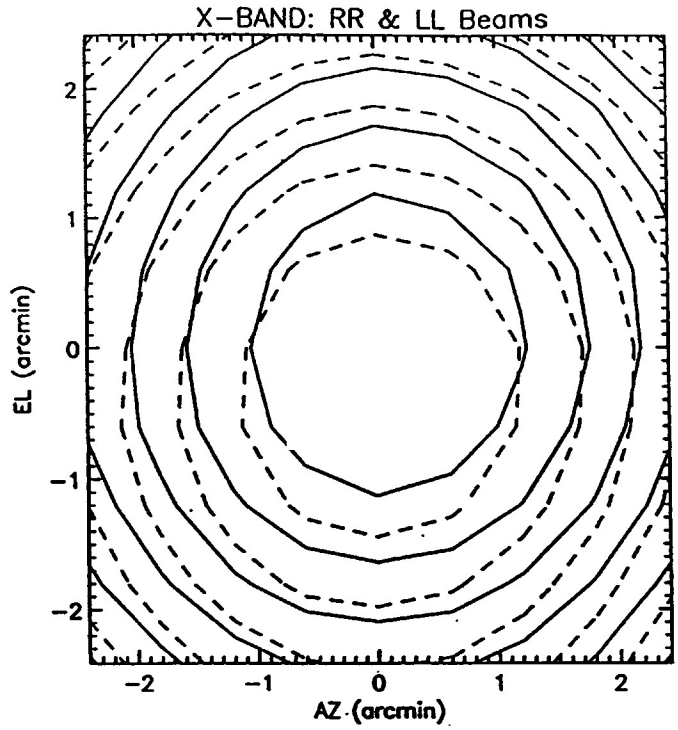

a)

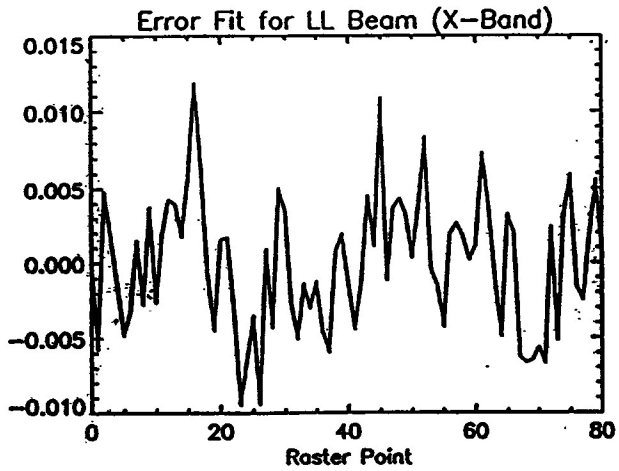

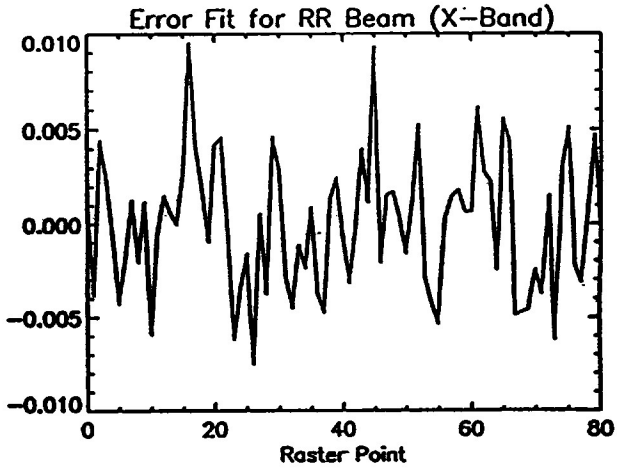

b)

Figure 3: (a) Circular Polarization beams for X-Band. (b) Normalized error for LL and RR beams.

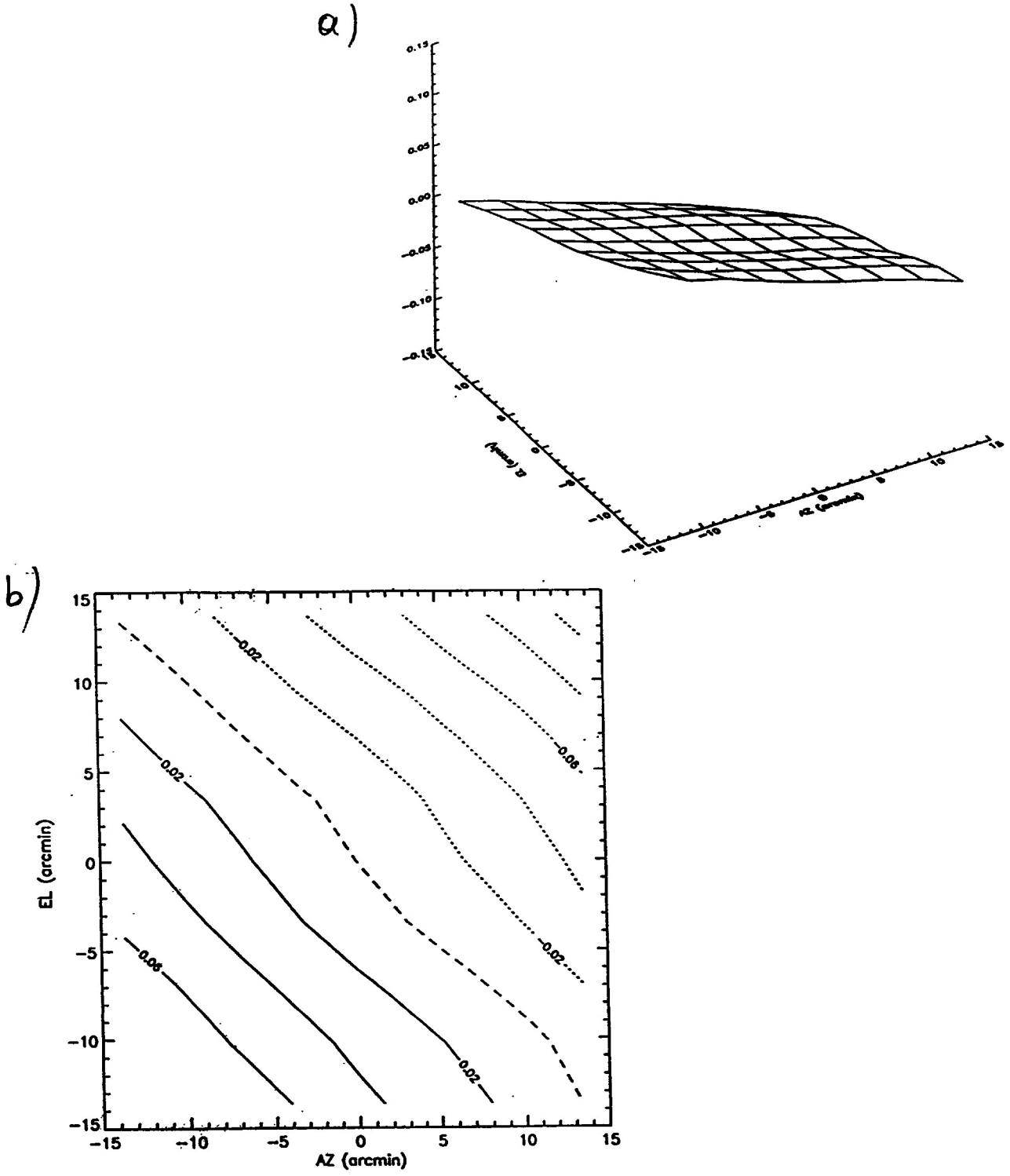

Figure 4: (a) Measured degree of circular polarization, ρ_c, surface for L band. (b) Contour plot of the same quantity in steps of 1% (*full line*: RCP; *dotted*: LCP; *dashed*: Zero Polarization).

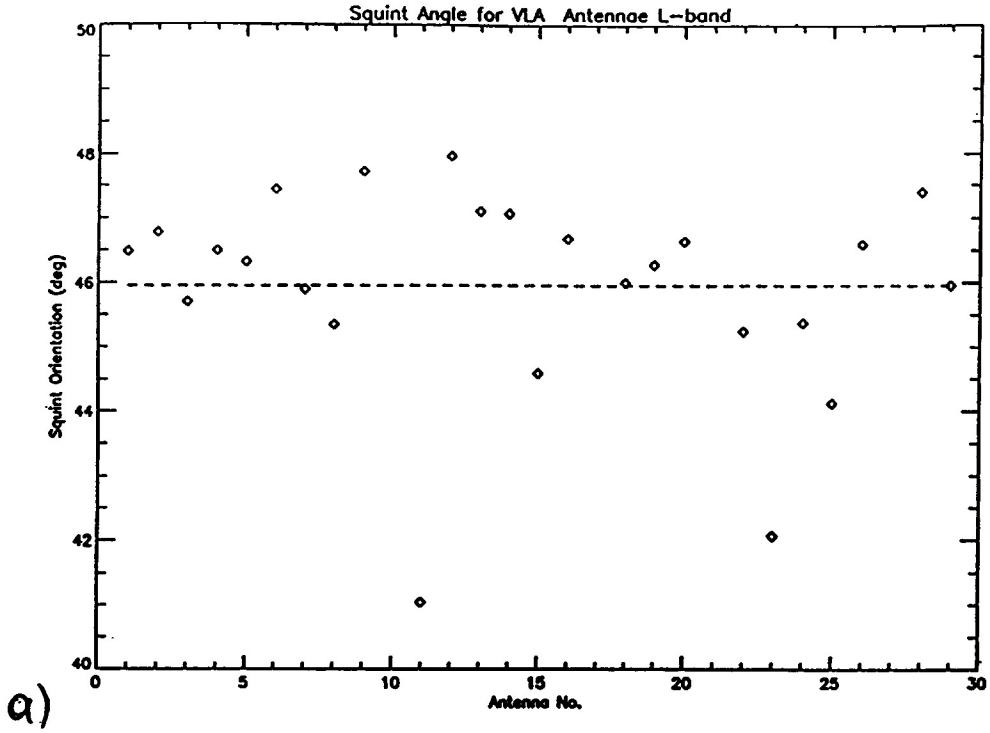

a)

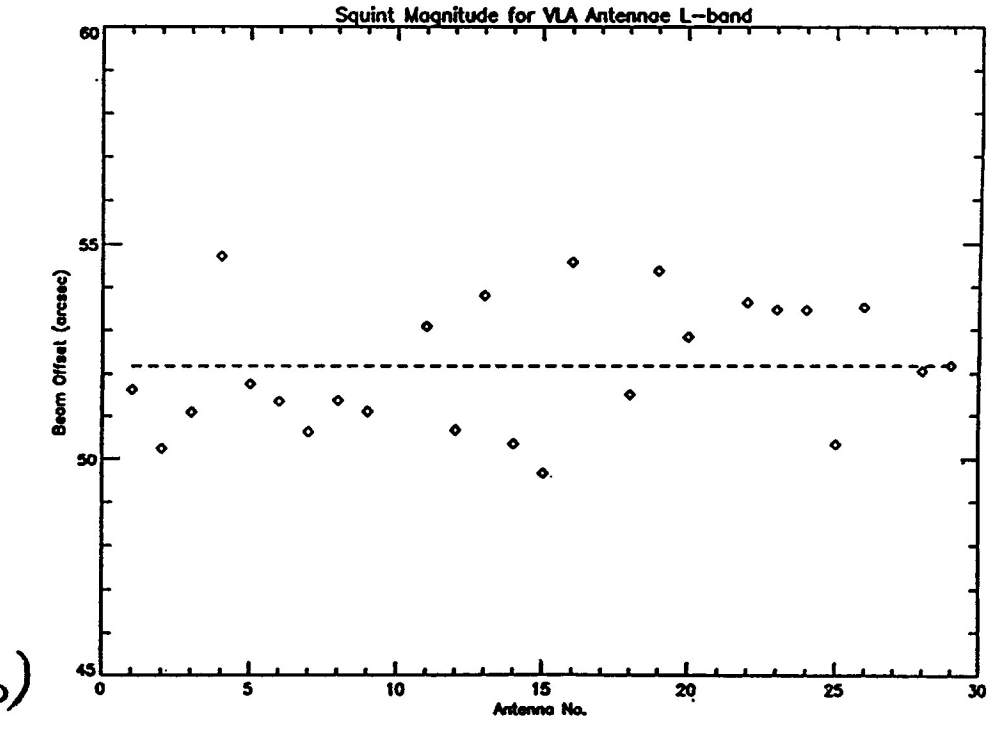

b)

Figure 5: (a) Squint angle for each VLA antenna (antennas 10,17,21 & 27 were flagged) for 1.4 GHz. The dashed line represents the average squint angle. (b) Squint magnitude for the same set of VLA antennas. The dashed line is the average offset.

a)

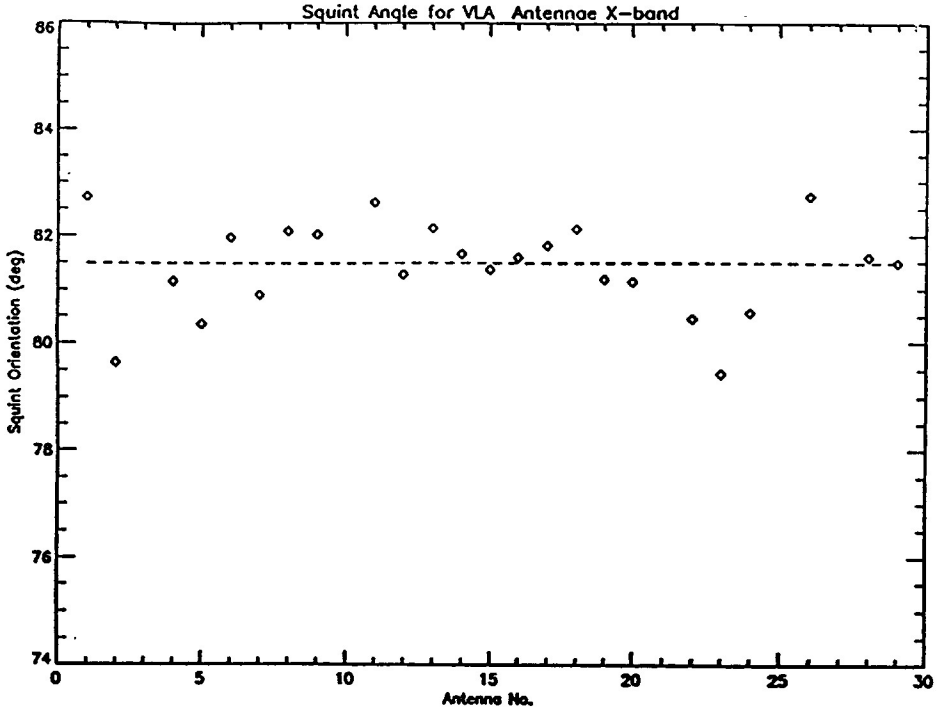

b)

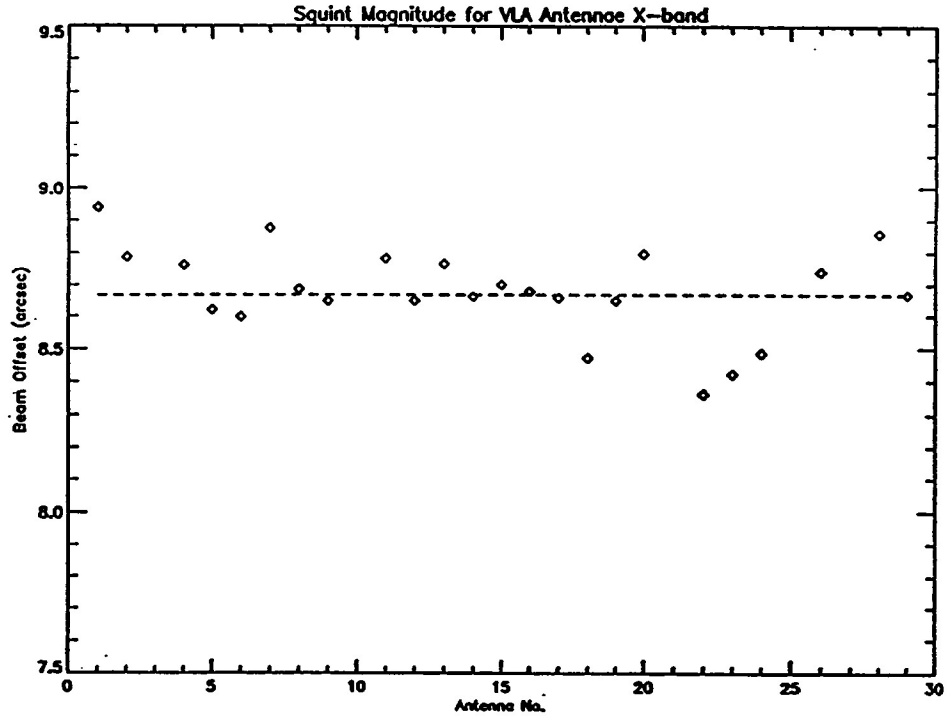

Figure 6: (a) Squint angle for each VLA antenna (antennas 3,10,17,21 & 27 were flagged) for 8.4 GHz. The dashed line represents the average squint angle. (b) Squint magnitude for the same set of VLA antennas. The dashed line is the average offset.

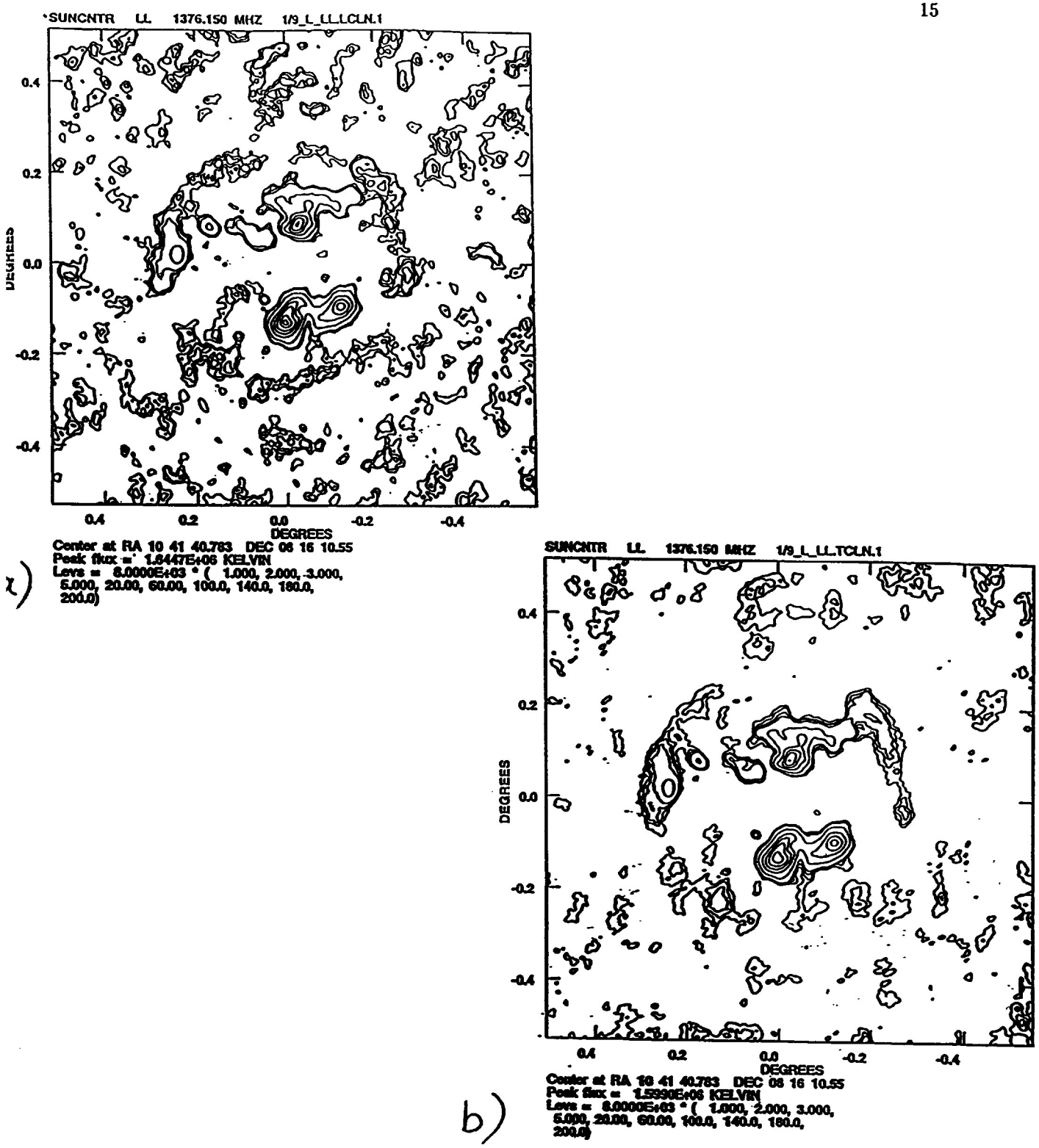

Figure 7: (a) Contour maps of stokes I 1.4 GHz image before squint correction. The contour levels are shown in the image (1σ = 8000 K). (b) The same map after the algorithm was applied. The contour levels are the same.